

# Prostate Imaging: Cancer AI (PI-CAI) Challenge 2022

## Z-SSMNet: A Zonal-aware Self-Supervised Mesh Network for Prostate Cancer Detection and Diagnosis in bpMRI

Yuan Yuan<sup>1</sup>, Euijoon Ahn<sup>2</sup>, Dagan Feng<sup>1,3</sup>, Mohamad Khadra<sup>4</sup>, Jinman Kim<sup>1</sup>

<sup>1</sup> School of Computer Science, University of Sydney, Sydney, Australia

<sup>2</sup> College of Science & Engineering, James Cook University, Cairns, Australia

<sup>3</sup> Med-X Research Institute, Shanghai Jiao Tong University, Shanghai, China

<sup>4</sup> Department of Urology, Nepean Hospital, Kingswood, Australia

### Abstract

Prostate cancer (PCa) is one of the most prevalent cancers in men and many people around the world die from ‘clinically significant’ PCa (csPCa). Early diagnosis of csPCa in bi-parametric MRI (bpMRI), which is non-invasive, cost-effective, and more efficient compared to multiparametric MRI (mpMRI), can contribute to precision care for PCa. The rapid rise in artificial intelligence (AI) algorithms are enabling unprecedented improvements in providing decision support systems that can aid in csPCa diagnosis and understanding. However, existing state of the art AI algorithms which are based on deep learning technology are often limited to 2D images that fails to capture inter-slice correlations in 3D volumetric images. The use of 3D convolutional neural networks (CNNs) partly overcomes this limitation, but it does not adapt to the anisotropy of images, resulting in sub-optimal semantic representation and poor generalization. Furthermore, due to the limitation of the amount of labelled data of bpMRI and the difficulty of labelling, existing CNNs are built on relatively small datasets, leading to a poor performance. To address the limitations identified above, we propose a new Zonal-aware Self-supervised Mesh Network (Z-SSMNet) that adaptatively fuses multiple 2D/2.5D/3D CNNs to effectively balance representation for sparse inter-slice information and dense intra-slice information in bpMRI. A self-supervised learning (SSL) technique is further introduced to pre-train our network using unlabelled data to learn the generalizable image features. Furthermore, we constrained our network to understand the zonal specific domain knowledge to improve the diagnosis precision of csPCa. Experiments on the PI-CAI Challenge dataset demonstrate our proposed method achieves better performance for csPCa detection and diagnosis in bpMRI. The Area Under the Receiver Operating Characteristics curve (AUROC) score and Average Precision (AP) score are 0.890 and 0.709 in Hidden Validation and Tuning Cohort (100 cases) (2<sup>nd</sup> rank) as well as 0.881 and 0.633 in Hidden Testing Cohort (1000 cases) (1<sup>st</sup> rank), respectively.

**Keyword:** Prostate cancer, Deep learning, Self-supervised learning, Bi-parametric MRI, PI-CAI 2022

### I. Introduction

According to the latest statistics of International Agency for Research on Cancer, prostate cancer (PCa) is the 2<sup>nd</sup> most commonly occurring cancer in men and the 4<sup>th</sup> most common cancer overall. Worldwide, an estimated 1,414,259 people (contributing 7.3% of new cancer cases) were diagnosed with PCa and an estimated 375,304 people (contributing 3.8% of new

cancer deaths) died from PCa in 2020 [1]. In the cancer statistics 2022 of American Cancer Society, the 5-year relative survival rate for patients diagnosed with local- or regional-stage PCa approaches 100% while for those diagnosed with the distant metastasis stage drops to 31% [2]. Finding ‘clinically significant’ PCa (csPCa) in early stage has a pivotal role in improving the survival rate of PCa and the quality of life for patients. However, reliable early warning clinical signs or symptoms are rarely produced in PCa [3]. Serum prostate-specific antigen (PSA) test are widely used in routine screening of PCa. While it’s controversial since the notorious overdiagnosis problem which can lead to overtreatments that have side effects such as urinary incontinence and erectile dysfunction [4]. Digital rectal examination (DRE) optionally following the abnormally elevated PSA is not recommended either due to low sensitivity and specificity as well as embarrassment and discomfort for the patient [5]. In the 2019 European Association of Urology (EAU) guidelines and the 2019 UK National Institute for Health and Care Excellence (NICE) guidelines, multiparametric magnetic resonance imaging (mpMRI) is recommended as the initial diagnostic test prior to biopsy to screen for high risk csPCa and localize the possible lesions [6, 7].

mpMRI of the prostate is mainly composed of anatomical T2-weighted imaging (T2WI) and the functional sequences of diffusion-weighted imaging (DWI) and dynamic contrast-enhanced (DCE) sequences. T2WI with superior soft-tissue resolution provides anatomical structural information and appears hypointense in lesion areas. DWI quantifies the degree of random movement of water molecules within tissue and shows hyperintense in lesion areas where the cellularity is higher. Conversely, the apparent diffusion coefficient (ADC) map quantifying the degree of diffusion restriction shows low signal in lesion areas. DCE (perfume imaging) involves the injection of a gadolinium (Gd)-based contrast media and can identify angiogenesis within the tumour microenvironment, which has a higher degree of contrast enhancement than normal vessels [8]. To promote global standardization in the interpretation of prostate mpMRI examinations, the European Society of Urogenital Radiology (ESUR) created the Prostate Imaging Reporting And Data System version 1 (PI-RADS v1) in 2012 and then it was updated to version 2 in 2015 and version 2.1 in 2019 [9]. Despite such standardization, the inter-reader agreement in diagnosis can be low (<50%) when the radiologists are inexperienced [10, 11] and the interpretation can be sub-optimal. And since this system is semi-quantitative, it is easily affected by radiologists’ subjective perception and image quality. Besides, considering the Gd-related adverse effects (Gd-brain deposits and nephrotoxicity) in DCE and the long imaging time which are not suitable for routine screening, bi-parametric MRI (bpMRI), excluding DCE, is evaluated for csPCa detection and the performance is comparable to mpMRI [12].

The prosperity of deep learning algorithms (a subset of AI) has promoted the realization of fully quantitative computer-aided detection and diagnosis (CAD) of PCa in mpMRI [13, 14]. In particular, the establishment of models based solely on bpMRI has become most popular among the community [15-17]. However, these methods are often limited to 2D images that fail to capture inter-slice correlations in 3D volumetric images [13, 16, 18, 19]. The use of 3D CNNs partly overcomes this limitation but it introduces interpolation artifacts and adds computational load when converting the image to isotropic dimensions (image resolution) to capture even physical receptive field [20]. Some works dealt with the in-plane and through-plane resolution differences of images in the network. They first reduced the intra-slice resolution to a level similar to the inter-slice resolution through anisotropic pooling or stride convolution, and then performed 3D convolutions on the roughly isotropic features [15, 21]. This does not fully adapt to the anisotropy of images, resulting in sub-optimal information representation and poor generalization ability. Besides, due to the limitation of the amount of data and the difficulty of labelling, the existing models are usually built on a relatively small

dataset from single centre, leading to a poor performance of the stability and generalization of the model [22].

Prostate Imaging: Cancer AI (PI-CAI), an all-new grand challenge with over 10,000 carefully-curated prostate MRI exams, is held to validate modern machine learning (ML) algorithms and estimate radiologists’ performance at csPCa detection and diagnosis [23]. For ML researchers, the main task is to build a model for lesion-level detection and patient-level diagnosis of csPCa in bpMRI. For this challenge, we have developed a Zonal-aware Self-supervised Mesh Network (Z-SSMNet) that adaptatively fuses multiple 2D/2.5D/3D CNNs to effectively balance representation for sparse inter-slice information and dense intra-slice information in bpMRI. A self-supervised learning (SSL) technique is also introduced to pre-train our network using unlabelled data to learn the generalizable image features. Furthermore, we constrained our network to understand the zonal specific domain knowledge to further improve the diagnosis precision of csPCa.

## II. Methods

The overview of our Z-SSMNet model is shown in Figure 1. We adopted a mesh network as the backbone and early fused the zonal anatomy information into the network to assist its learning. We also introduced an SSL technique to pre-train the network without labels and then fine-tuned it with labelled data. It mainly consists of three parts: 1) zonal mask generation; 2) self-supervised pre-training of the mesh network; 3) fine-tuning of the network for csPCa detection and diagnosis in bpMRI.

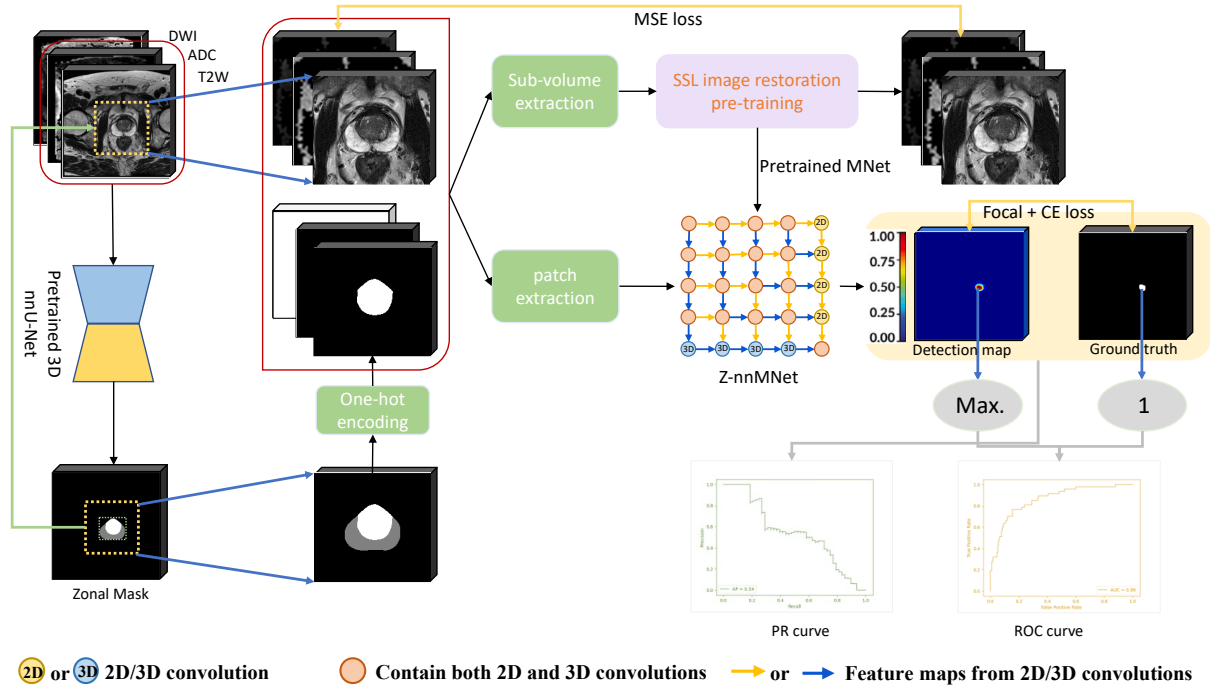


**Figure 1.** The overview of our Z-SSMNet model consisting of three main parts: 1) zonal mask generation; 2) self-supervised pre-training of the mesh network; 3) fine-tuning of the mesh network for csPCa detection and diagnosis in bpMRI.

### 1. Zonal-aware Self-supervised Mesh Network (Z-SSMNet)

Our Z-SSMNet was built based on the network from [24] which seriously considers the anisotropy of medical images and latently fuses the multi-dimensional convolutions to

adaptively balance the representation for sparse inter-slice information and dense intra-slice information. Multimodal bpMRI images (T2WI, ADC, DWI) were input to three channels of the network. Considering the differences of frequency and imaging appearance of prostate lesions in peripheral zone (PZ) and transition zone (TZ) [25], we input the one-hot encoded zonal mask to the other three channels to guide the network to learn zonal specific knowledge. The network was pre-trained first in an SSL manner and then fine-tuned with labels for csPCa detection and diagnosis.

## 2. Zonal Mask Generation

We trained a standard 3D nnU-Net [26] model with T2WI and ADC images from 3 public datasets to generate prostate zonal segmentation mask (PZ and TZ). The mask was used to guide the network to learn region-specific high-level semantic information and assist in cropping of the regions of interest (ROI). We also removed noisy markers outside the prostate region as part of a post-processing method. Then we cropped the images and masks with the region of the prostate’s bounding box, expanding 2.5cm outward in all directions as the ROI. This allows for tumour outgrowth of the prostate and preserves a clear outline of the prostate relative to adjacent tissues and organs.

## 3. Self-supervised Pre-training of the Mesh Network

We used the image restoration of learning fine-grained pixel-level information as a pretext task and pre-trained our network in a self-supervised manner. Four specially tailored data augmentation methods were used in the image restoration task: 1) non-linear transformation by recovering the intensity values of the images that have undergone a set of monotonically non-linear transformations. The model learns the appearance of the anatomic structures present in the images, 2) local shuffling by guiding the model to learn rich local texture and boundary information of objects while keeping its global structure understandable, 3) inner-cutout which learns the local continuous of organs and 4) outer-cutout which learns the organ spatial layout and global geometry. The detailed descriptions of data augmentation methods are also available in [27].

## 4. csPCa Detection and Diagnosis in bpMRI

The pre-trained mesh network was then fine-tuned using labelled data for csPCa detection and diagnosis. Considering the heterogeneous between data from multi-centres and multi-vendors, we integrated the pre-trained network into the famous nnU-Net framework to form the Z-nnMNet that can pre-process the data adaptively. We performed the same pre-processing and augmentation on the zonal mask as the tumour label. The loss function consists of focal loss and cross-entropy loss. The generated detection map was post-processed by dynamic lesion extraction method proposed by Bosma et al. [21]. And the maximum value of its pixels was regarded as the predicted probability of the patient-level diagnosis.

# III. Experiments

## 1. Datasets

*PI-CAI Dataset:* provided by the challenge organizers including three Dutch centers (Radboud University Medical Center (RUMC), Ziekenhuis Groep Twente (ZGT), University Medical Center Groningen (UMCG)) and one Norwegian center (Norwegian University of Science and Technology (NTNU)), this dataset is sampled into four splits: 1) Public Training and Development Dataset. 2) Private Training Dataset. 3) Hidden Validation and Tuning Cohort. 4) Hidden Testing Cohort. There are 1500 cases in the Public Training and Development Dataset, including 328 cases from the ProstateX Challenge. Among them, 1075 cases have benign tissue or indolent PCa labelled as all zero, 220 malignant cases are manual labelled by one of 10 trained investigators or 1 radiology resident, under supervision of one of 3 expert radiologists, at RUMC, UMCG or NTNU. Each annotation is derived using all available MRI scans, diagnostic reports (radiology, pathology) and whole-mount

prostatectomy specimen (if applicable). The other 205 malignant cases are labelled by an AI model. All original annotations are converted to the same dimensions and spatial resolution as their corresponding T2WI images. There are 7607 cases in the Private Training Dataset, 100 cases in the Hidden Validation and Tuning Cohort used for a live, public leaderboard that enables model selection and tuning, and 1000 cases in the Hidden Testing Cohort used to benchmark the AI algorithms at the end of Closed Testing Phase. Institutional review boards of all four centres have waived the need for informed patient consent. For all the patients, bpMRI scans (including Axial T2WI, Axial high b-value ( $\geq 1000$  s/mm<sup>2</sup>) DWI, Axial ADC acquired using Siemens Healthineers or Philips Medical Systems-based scanners with surface coils are offered. In the first round of the challenge, we used the 1500 cases in the Public Training and Development Dataset for model training.

*ProstateX dataset:* Although the ProstateX dataset is included in PI-CAI dataset, no zonal masks are provided. Based on the original ProstateX dataset [28], Cuocolo et al. [29] labelled the lesion masks and zonal masks of the data to promote the prostate related researches like lesion detection and zonal segmentation. We used the 204 cases in ProstateX with zonal mask labels for the nnU-Net model training for zonal mask segmentation.

*Prostate158 dataset:* Prostate158 including 158 cases is a curated dataset of 3 Tesla prostate bpMRI images for automatic segmentation of anatomical zones and carcinomatous lesions. Histopathologic confirmation is available for each cancerous lesion. All studies include a T2WI and DWI images with ADC maps. Images in each study were resampled so that orientation, direction, and spacing were the same [20]. We used this dataset in the zonal mask segmentation model training stage, SSL pre-training stage and csPCa detection stage.

*MSD prostate dataset:* This dataset consists of 48 prostate mpMRI studies comprising T2WI, DWI and DCE series. A subset of two series, transverse T2WI and the ADC was selected. The corresponding target ROIs were the prostate PZ and TZ. The data was acquired at Radboud University Medical Centre [30]. We only used 32 cases in the public training dataset for training the zonal mask segmentation model.

## 2. Experiment Details

*Data pre-processing:* All the data are transferred to NifTI format and then resampled to same dimensions and spatial resolution as their corresponding original T2WI images. 394 cases coming from the Prostate158 dataset, ProstateX dataset and MSD prostate dataset with T2WI and ADC modalities were used for zonal segmentation model training. The PI-CAI dataset and Prostate158 dataset were combined to train the Z-SSMNet. For the SSL pre-training, all the data were first resampled to 0.5x0.5x3 mm, T2WI and DWI images were normalized to [0, 1] by the min-max normalization and the intensity values in each ADC map were clipped within the range of [0, 3000] and then normalized to [0, 1].

*Implementation details:* When training the zonal mask segmentation model, we used T2WI and ADC as input, and the ratio of the training set to the test set is 4:1. The zonal mask generated by the trained model is post-processed to remove the noisy markers in extra-prostatic area and then used as additional input channels for Z-SSMNet. For the pretext task of SSL pre-training, we extracted 3D sub-volumes with the size of 64x64x16 from each case as input and the ratio of the training set to the test set is 4:1. The stochastic gradient descent (SGD) with a momentum of 0.9 is selected as the optimizer. The initial learning rate (0.1) is gradually reduced according to the step learning rate policy. The loss function is mean squared error (MSE) loss. It should be noted that we do not change the zonal mask when performing nonlinear transformation on the images. In addition, inner-cutout and outer-cutout are mutually exclusive when used. The augmented zonal mask is one-hot encoded before being input into the network. For the csPCa detection and diagnosis, the cropped bpMRI mainly including the prostate area and the corresponding mask are input into the network. The PI-CAI dataset adopts the five-fold cross-validation split method provided by the organizer, and the Prostate158

dataset is randomly added to each fold after stratification. The initial learning rate (0.01) is gradually reduced according to the “poly” learning rate policy and the maximum of epoch is setting to 500. The loss function is combined focal loss and cross-entropy loss.

### 3. Evaluation Metrics

Patient-level diagnosis performance is evaluated using the Area Under Receiver Operating Characteristic (AUROC) metric. Lesion-level detection performance is evaluated using the Average Precision (AP) metric. Overall score used to rank each AI algorithm is the average of both task-specific metrics:

$$\text{Overall Ranking Score} = (\text{AP} + \text{AUROC}) / 2.$$

## IV. Results

Our test results on the PI-CAI Hidden Validation and Tuning Cohort and Hidden Testing Cohort are shown in Table 1.

**Table 1.** The test results of our Z-SSMNet model.

Dataset	Ranking Score	AUROC	AP
Hidden validation and tuning cohort	0.800	0.890	0.709
Hidden testing cohort	0.757	0.881	0.633

## V. Conclusion

We proposed a zonal-aware self-supervised mesh network (Z-SSMNet) for csPCa detection and diagnosis in bpMRI data. Our model implicitly fuses the multi-dimensional features in a balanced way by deep latent fusion of 2D/2.5D/3D convolutions which adapting to the variation of spacing ratios inter axes. The model for zonal mask segmentation was pre-trained on T2WI and ADC images. By fusing the zonal information into the model and pre-training the backbone with self-supervised learning which leveraging the availability of large amounts of unlabelled data, our model outperformed other competing algorithms, with 2<sup>nd</sup> ranking score of 0.800 in the hidden validation and tuning cohort and highest ranking score of 0.757 in the hidden testing cohort.

## References

- [1] H. Sung, J. Ferlay, R. L. Siegel *et al.*, “Global cancer statistics 2020: GLOBOCAN estimates of incidence and mortality worldwide for 36 cancers in 185 countries,” *Ca-a Cancer Journal for Clinicians*, vol. 71, no. 3, pp. 209-249, May, 2021.
- [2] R. L. Siegel, K. D. Miller, H. E. Fuchs *et al.*, “Cancer statistics, 2022,” *Ca-a Cancer Journal for Clinicians*, vol. 72, no. 1, pp. 7-33, Jan, 2022.
- [3] P. Rawla, “Epidemiology of Prostate Cancer,” *World Journal of Oncology*, vol. 10, no. 2, pp. 63-89, Apr, 2019.
- [4] D. C. Grossman, S. J. Curry, D. K. Owens *et al.*, “Screening for Prostate Cancer US Preventive Services Task Force Recommendation Statement,” *Jama-Journal of the American Medical Association*, vol. 319, no. 18, pp. 1901-1913, May 8, 2018.
- [5] L. Naji, H. Randhawa, Z. Sohani *et al.*, “Digital Rectal Examination for Prostate Cancer Screening in Primary Care: A Systematic Review and Meta-Analysis,” *Annals of Family Medicine*, vol. 16, no. 2, pp. 149-154, Mar-Apr, 2018.
- [6] “EAU Guidelines on Prostate Cancer,” 2019.
- [7] “NICE Guidance - Prostate cancer: diagnosis and management (c) NICE (2019) Prostate cancer: diagnosis and management,” *Bju International*, vol. 124, no. 1, pp. 9-26, Jul, 2019.

- [8] A. Stabile, F. Giganti, A. B. Rosenkrantz *et al.*, “Multiparametric MRI for prostate cancer diagnosis: current status and future directions,” *Nature Reviews Urology*, vol. 17, no. 1, pp. 41-61, Jan, 2020.
- [9] R. T. Gupta, K. A. Mehta, B. Turkbey *et al.*, “PI-RADS: Past, present, and future,” *J Magn Reson Imaging*, vol. 52, no. 1, pp. 33-53, Jul, 2020.
- [10] A. B. Rosenkrantz, L. A. Ginocchio, D. Cornfeld *et al.*, “Interobserver Reproducibility of the PI-RADS Version 2 Lexicon: A Multicenter Study of Six Experienced Prostate Radiologists,” *Radiology*, vol. 280, no. 3, pp. 793-804, Sep, 2016.
- [11] A. C. Westphalen, C. E. McCulloch, J. M. Anaokar *et al.*, “Variability of the Positive Predictive Value of PI-RADS for Prostate MRI across 26 Centers: Experience of the Society of Abdominal Radiology Prostate Cancer Disease-focused Panel,” *Radiology*, vol. 296, no. 1, pp. 76-84, Jul, 2020.
- [12] T. Tamada, A. Kido, A. Yamamoto *et al.*, “Comparison of Biparametric and Multiparametric MRI for Clinically Significant Prostate Cancer Detection With PI-RADS Version 2.1,” *J Magn Reson Imaging*, vol. 53, no. 1, pp. 283-291, Jan, 2021.
- [13] Y. Song, Y. D. Zhang, X. Yan *et al.*, “Computer-aided diagnosis of prostate cancer using a deep convolutional neural network from multiparametric MRI,” *J Magn Reson Imaging*, vol. 48, no. 6, pp. 1570-1577, Dec, 2018.
- [14] O. J. Pellicer-Valero, J. L. Marenco Jimenez, V. Gonzalez-Perez *et al.*, “Deep learning for fully automatic detection, segmentation, and Gleason grade estimation of prostate cancer in multiparametric magnetic resonance images,” *Sci Rep*, vol. 12, no. 1, pp. 2975, Feb 22, 2022.
- [15] A. Saha, M. Hosseinzadeh, and H. Huisman, “End-to-end prostate cancer detection in bpMRI via 3D CNNs: Effects of attention mechanisms, clinical priori and decoupled false positive reduction,” *Med Image Anal*, vol. 73, pp. 102155, Oct, 2021.
- [16] J. Hu, A. Shen, X. Qiao *et al.*, “Dual attention guided multi-scale neural network trained with curriculum learning for noninvasive prediction of Gleason grade groups from MRI,” *Med Phys*, Nov 22, 2022.
- [17] C. Vente, P. Vos, M. Hosseinzadeh *et al.*, “Deep Learning Regression for Prostate Cancer Detection and Grading in Bi-Parametric MRI,” *IEEE Trans Biomed Eng*, vol. 68, no. 2, pp. 374-383, Feb, 2021.
- [18] R. M. Cao, A. M. Bajgirani, S. A. Mirak *et al.*, “Joint Prostate Cancer Detection and Gleason Score Prediction in mp-MRI via FocalNet,” *Ieee Transactions on Medical Imaging*, vol. 38, no. 11, pp. 2496-2506, Nov, 2019.
- [19] X. Yu, B. Lou, B. B. Shi *et al.*, “False Positive Reduction Using Multiscale Contextual Features for Prostate Cancer Detection in Multi-Parametric Mri Scans,” *2020 Ieee 17th International Symposium on Biomedical Imaging (Isbi 2020)*, pp. 1355-1359, 2020.
- [20] L. C. Adams, M. R. Makowski, G. Engel *et al.*, “Prostate158 - An expert-annotated 3T MRI dataset and algorithm for prostate cancer detection,” *Comput Biol Med*, vol. 148, pp. 105817, Sep, 2022.
- [21] Joeran Bosma, Anindo Saha, Matin Hosseinzadeh *et al.*, “Semi-supervised learning with report-guided lesion annotation for deep learning-based prostate cancer detection in bpMRI,” *arXiv:2112.05151*, 2021.
- [22] M. R. S. Sunoqrot, A. Saha, M. Hosseinzadeh *et al.*, “Artificial intelligence for prostate MRI: open datasets, available applications, and grand challenges,” *Eur Radiol Exp*, vol. 6, no. 1, pp. 35, Aug 1, 2022.

- [23] A. Saha, J. J. Twilt, J. S. Bosma *et al.*, “Artificial Intelligence and Radiologists at Prostate Cancer Detection in MRI: The PI-CAI Challenge (Study Protocol) (1.0),” *Zenodo*, 2022.
- [24] Z. Dong, Y. He, X. Qi *et al.*, “MNet: Rethinking 2D/3D Networks for Anisotropic Medical Image Segmentation,” *arXiv:2205.04846*, 2022.
- [25] A. Ali, A. Du Feu, P. Oliveira *et al.*, “Prostate zones and cancer: lost in transition?,” *Nat Rev Urol*, vol. 19, no. 2, pp. 101-115, Feb, 2022.
- [26] F. Isensee, P. F. Jaeger, S. A. A. Kohl *et al.*, “nnU-Net: a self-configuring method for deep learning-based biomedical image segmentation,” *Nature Methods*, vol. 18, no. 2, pp. 203+, Feb, 2021.
- [27] Z. Zhou, V. Sodha, J. Pang *et al.*, “Models Genesis,” *Med Image Anal*, vol. 67, pp. 101840, Jan, 2021.
- [28] Geert Litjens, Oscar Debats, Jelle Barentsz *et al.*, “ProstateX Challenge data,” *The Cancer Imaging Archive*, 2017.
- [29] R. Cuocolo, A. Stanzone, A. Castaldo *et al.*, “Quality control and whole-gland, zonal and lesion annotations for the PROSTATEx challenge public dataset,” *European Journal of Radiology*, vol. 138, May, 2021.
- [30] M. Antonelli, A. Reinke, S. Bakas *et al.*, “The Medical Segmentation Decathlon,” *Nat Commun*, vol. 13, no. 1, pp. 4128, Jul 15, 2022.